# Accurate Dynamical Models of Interneuronal GABAergic Channel Physiologies

James B. Maciokas[1], Philip Goodman[2], John Kenyon[2],
Maria Toledo-Rodriguez[3], Henry Markram[4]

**Abstract**

Recent experimental results have revealed a large diversity of anatomic, synaptic and membrane physiology within the GABAergic system. By incorporating combinations of parametrically varied M-type, A-type, and calcium-dependent potassium (AHP) channels, we were able to replicate *in vitro* responses to 1-second current steps ranging from 50 to 350 pA. Our results show the need for subthreshold activating channels to capture the physiological properties of GABAergic cells. Presently underway is a collaboration among the authors to corroborate the proposed channel models using genetic profiles obtained from physiologically characterized interneurons.

*Keyword:* GABA, sub-threshold, channel, cortex

## 1 Background

The GABAergic system in the neocortex has been widely studied for it's anatomic, synaptic, and membrane physiology [1, 2]. Although these processes are of fundamental importance in understanding the GABAergic system little is know about the unique combination and sensitivity of these processes which lead to the diverse firing behavior seen in GABAergic neurons.

Recently [1] has shown that the behavior of neocortical interneurons was too diverse to be captured by the previous classifications of "fast-spiking," "bursting," and "regular spiking" [3]. By applying step current of varying intensities [1] was able to use *in vitro* recordings to further classify GABAergic cells. Given the growing evidence of the diversity of the GABAergic system across anatomic [2] [1], synaptic [1], and physiologic measures [3] [1] and given the ability to model synaptic dynamics [4] [5] the next logical step is to model the electro-physical behavior of the neocortical interneurons using various combinations of voltage-dependent or calcium-dependent potassium channels.

## 2 Methods

Simulations were performed using NeoCortical Simulator on a 34 node Beowulf system (dual 2.2-GHz Xeon processors, 4-GB ram, Myrinet 2000 interconnect) [6]. The frequency sampling value (FSV) was 10,000 ticks per second.

### 2.1 Model

Our point neuron model included resting potential (-70 to -65mV), threshold (-40 to -35mV), spike template, resistance (200 Mohms), $E_k$ (-80mV), calcium spike increment (160 to 260nM), and calcium tau (70ms) based on published data [1] [7]. We used combinations of linked differential equations modified from [9] for M-type (non-inactivating), [8] for A-type (sub threshold inactivating), [9] for calcium-dependent potassium (SK), and proposed settings for SIC (suprathreshold inactivating) channels (Figure 1-4). Simulations were run with 1.5-second current steps ranging from 150 to 300 pA.

### 2.2 SK-type channel

We chose an SK-type channel as our $Ca^{+2}$ dependent $K^+$ channel (Figure 1a) for our model due to the increasing evidence that such a channel determines spike frequency adaptation [10]. Further evidence

[1] Center for Neuroscience, University of California, Davis (USA) – jbmaciokas@ucdavis.edu

[2] Internal Medicine and Biomedical Engineering, University of Nevada (USA)

[3] Brain and Mind Institute, EPFL (Switzerland) and Dept. of Neurobiology, Weizmann Institute of Science (Israel)

[4] Brain and Mind Institute, EPFL (Switzerland)

suggests that BK-type channels are activated only under pathological conditions [11] and therefore were not included in our model. Our AHP channel was modeled after [9].

### 2.3 A-type channel

Since successful modeling of AP in squid giant axon in [12], a transient $K^+$ current has been linked to AP repolarization and spike frequency modulation in mammalian cells in addition to the delayed rectifier [13]. Two types of transient $K^+$ channels have been linked to AP repolarization and/or spike frequency modulation: a fast opening, extremely brief ($K_f$) channel and a longer opening ($K_A$) channel [11]. For purposes of our model, the $K_f$ channel was not needed to aid in AP repolarization due to use of a spike-template for our AP. The $K_A$ channel, which has a longer lasting effect relative to the $K_f$ channel, was included in our model because its effect can be felt during interspike intervals. The $K_A$ channel works like a "shock absorber", activating across hyperpolarized potentials in order to prevent small fluctuations in current from reaching threshold and then inactivating with a slower time constant during spike train sequences [8] [14]. A-channel dynamics were based on [8].

### 2.4 M-type channel

The M-current initially described in bullfrog sympathetic ganglion [15] has been found in many central nervous system neurons [16, 17] and is characterized by a slowly activating and deactivating conductance linked to sub threshold responsiveness [18] [9]. Our M-type channel dynamics were based from [19].

### 2.5 SIC channel

A suprathreshold inactivating channel was derived to obtain complex stuttering behavior found in an extremely small proportion of neocortical interneurons. The SIC channel was modified from an A-type channel to activate after spiking occurs, preventing continued spiking, and then inactivates allowing spiking to occur again. Traditional A-type channels open up sub-threshold and contribute to more of a delayed behavior.

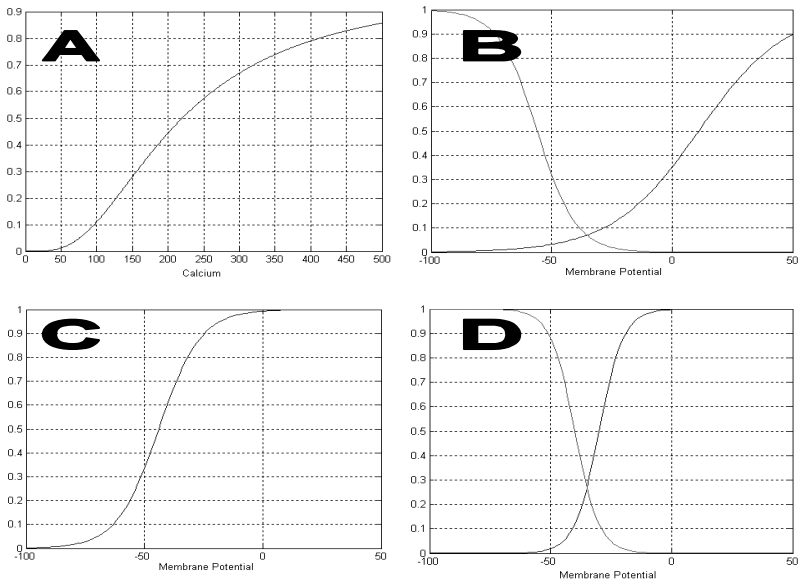


Figure 1: Activation and/or inactivation curves of the channels used in the models. (a) Calcium-dependent activation curve for SK-type channel with a half min of 220nM. (b) Activation and inactivation curves for the A-type channel with a half min of 11mV and –56mV and a slope factor of 18 and 8 for the m-particle and h-particle respectively. (c) Activation curve for M-type channel with a half min of –44mV and a slope factor of 8.8. (d) Activation and inactivation curves for proposed SIC type channel with a half min of –30mV and –40mV and a slope factor of 5 for the m-particle and h-particle respectively.

### 2.6 cNAC model

Recent evidence has shown that AP repolarization is not $Ca^{2+}$ dependent [20] and that voltage-gated $K^+$ channels, not $Ca^{2+}$ activated $K^+$ channels, are largely responsible for AP repolarization [13] [21] [22]. In addition models of M-type channels [9] and SK channels [10] have been shown to contribute to spike frequency adaptation. In contrast, A-type channels have been linked to neuronal repetitive firing without accommodation [23] [24] [25]. In light of this evidence we used only an A-type channel to model cNAC behavior.

### 2.7 bNAC model

Whole cell recordings display a cell that bursts with stimulus onset and then rapidly settles into a steady state [1]. This type of behavior cannot be achieved with an A-type channel or an M-type channel. What is needed is a channel that allows several quickly occurring spikes before reacting. Past reports suggest that there is a fast calcium-dependent $K^+$ current [26] [25]. We modeled bNAC behavior by using a fast calcium-dependent potassium channel with a tau scale factor of 0.2 and a calcium spike increment of 260nM.

### 2.8 dNAC model

A higher threshold (-35mV) was used to stay consistent with biological data on dNAC type cells. For similar reasons as those for our cNAC model, we used only an A-type channel to model the delayed behavior. The A-type channel was modified from [8] to achieve the delayed behavior. The time constants for the h-particle were increased from 5ms to 100ms for membrane potentials < -20mV and were increased likewise for the membrane potentials > -20mV. The time constants for the m-particle were unchanged as were the halfmins for the m and h particles.

### 2.9 cAC model

As mentioned before, models of M-type channels [9] and SK channels [10] have been shown to contribute to spike frequency adaptation and therefore were included to achieve cAC behavior. Previous reports have shown that several after-hyper-polarizations occur following an AP: a fast ($I_C$) calcium dependent current, an intermediate non-calcium dependent current, and a slow ($I_{AHP}$) calcium dependent current [25]. Our cAC model included M-type, fast (tau scale factor 0.01) and slow (tau scale factor 5.0) calcium dependent potassium channels in the ratio 1:1:2 respectively.

### 2.10 bAC model

Our bAC model included two SK channels without an M-channel. An M-channel opens up subthreshold, preventing bursting to occur despite its gradual opening and closing. The SK channels were similar to cAC settings with the exception that the fast SK channel is slightly slower to respond (tau scale factor 0.2) allowing an initial burst. We used a ratio of one fast SK-type channel to two slow SK-type channels.

### 2.11 dAC model

For similar reasons as those given for our cAC model, the dAC model included an M-type channel and fast and slow calcium-dependent potassium channels with the same settings to achieve accommodating behavior once spiking occurs. An A-type channel like the one used in our dNAC model was included to achieve delayed behavior. The ratio of an M-type channel, fast & slow calcium-dependent potassium channels and A-type channels was 1:1:2:25, respectively.

### 2.12 cSTUT/bSTUT model

Our cSTUT model included a SIC channel derived from observation of whole recordings of stuttering behavior. What was needed was a channel that activates once spiking occurs (suprathreshold), suppressing further spikes, and then inactivates with a delay, allowing spiking to occur again. The bSTUT model was similar to the cSTUT model with the exception that the h-particle has a slightly slower time constant, allowing an initial burst to occur.

## 3 Results

### 3.1 cNAC Behavior

In Figure 2a one can see that the steady-state firing frequency is reached simultaneously with stimulus onset characteristic of cNAC behavior. The m-particle tracks m-infinity nearly 1:1, and the h-particle lags slightly behind h-infinity, minimizing but not eliminating the effect of the channel once spiking occurs.

### 3.2 bNAC Behavior

Observe the characteristic initial burst followed immediately by a steady-state firing frequency (Figure 2c). With a tau of ~5ms, the channel opens slightly slower upon $Ca^{+2}$ entry from an action potential. In this case several spikes occur before the channel opens sufficiently enough to suppress firing and settle into a steady state.

### 3.3 dNAC Behavior

Notice the initial delay followed right away by a steady-state firing frequency typical of dNAC behavior (Figure 2e). The delay is due to a transient A-type channel with a substantial time constant for the inactivation component. The A-type channel opens up, suppressing spiking until the inactivation component catches up and shuts down the channel, allowing spiking to occur approximately 200ms after the stimulus onset. Decreasing the strength of the A-type channel in steps up to 120% yields increased firing frequency and shorter delays until spiking occurred immediately following stimulus onset. Increasing the strength of the channel up to 50% increases the delay and decreases the firing frequency until the channel is strong enough to keep the cell from reaching threshold.

### 3.4 cAC Behavior

The characteristic adapting spike pattern is readily seen in Figure 2b. The M-channel opens gradually, hyperpolarizing the cell and contributing to the accommodating pattern. The fast SK-type channel opens rapidly, having its maximum effect early. In contrast, the slow SK-type channel, with a time constant of ~1-2sec, opens late, having its maximum effect towards the end of the injected current.

### 3.5 bAC Behavior

The initial burst followed by the adapting spike rate is characteristic of bAC behavior (Figure 2d). Similar to the bNAC model, the fast SK-type channel has a tau of ~5ms, allowing several spikes to occur before fully reacting. The presence of the slow SK-type channel with a tau of ~1sec contributes to the accommodating behavior seen following the initial burst.

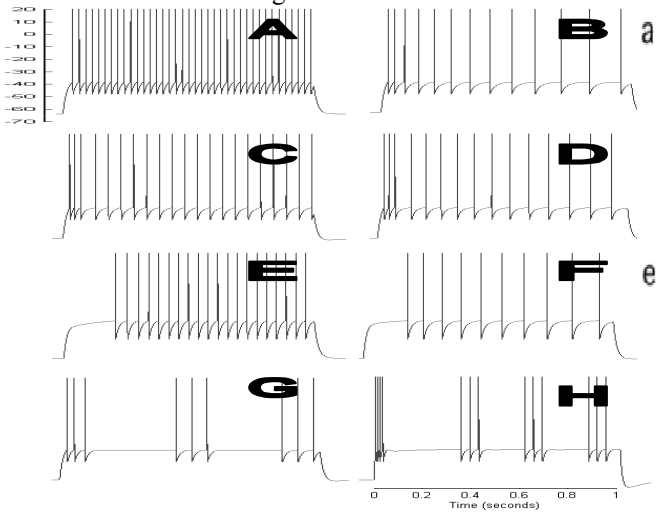


Figure 2: Simulated response to step current of 150-300 pA. A. classic non-accommodating (cNAC). B. classic accommodating (cAC). C. bursting non-accommodating (bNAC). D. bursting accommodating (bAC). E. delayed non-accommodating (dNAC). F. delayed accommodating (dAC). G. classic stuttering (cSTUT). H. bursting stuttering (bSTUT).

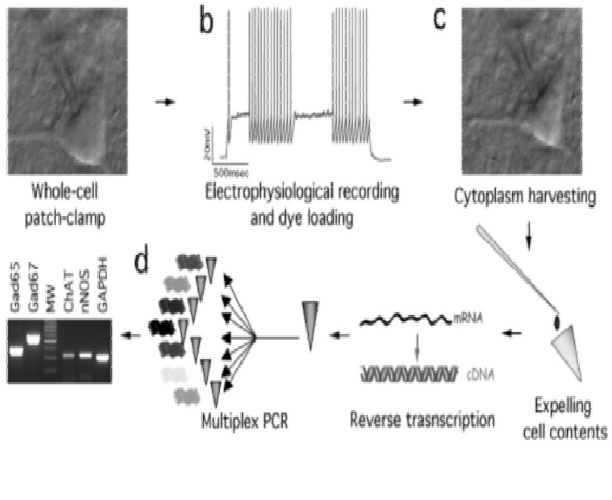


Figure 3: Single Cell multiplex RT-PCR technique used by the Markram laboratory (unpublished data). Whole-cell patch-clamp recordings from different classes of neocortical neurons are obtained from stimulation protocols. At the end of each recording the neuron's cytoplasm is extracted for multiplex RT-PCR. Simultaneous detection of many mRNAs is obtained from a positive control sample (typically , 250pg of total brain mRNA). These may include voltage activated K channels, calcium activated K channels, K/Na permeable hyperpolarization activated channels, voltage activated Ca channels, and cacium buffering proteins.

### 3.6 dAC Behavior

Delayed accommodating behavior (Figure 2f) was obtained using the same channel configuration found for cAC behavior with the addition of a transient A channel used in the dNAC settings. Once again, the delayed behavior is due to the long time constant for the inactivation component of the A-channel. The M-channel contributes to the delayed behavior due to its subthreshold activation. The calcium-dependent SK-type channels have no effect on the cell until spiking occurs.

### 3.7 cSTUT/bSTUT Behavior

Classic stuttering behavior (Fig 2g and 2h) was achieved by deriving a suprathreshold inactivating channel (SIC). The justification for such a channel was determined by the stuttering behavior itself. A channel was needed that is activated after spiking occurs, suppressing further spiking and then is inactivated with a delay, allowing spiking to occur again. Bursting stuttering behavior was modeled using a similar SIC channel used to obtain cSTUT; behavior, however the time constants for the h-particle was slightly slower. We were unable to achieve this complex behavior using combinations of A-type, M-type and/or SK-type channels. Stuttering-type cells represent only a small fraction of interneurons in the neocortex, and the modeled behavior was achieved under only a limited combination of stimulus strengths and channel dynamics.

## 4 Discussion

Defining the mechanisms that contribute to the diversity of firing patterns in the GABAergic system is of central importance in furthering our understanding of several key issues in neuroscience. Modeling cellular dynamics contributes to our understanding of the mechanisms required to achieve the diverse behavior. Our model makes use of M-type, A-type, SK-type and SIC channels to replicate *in vitro* responses [1].

In this series of simulations, we found that all behaviors except for “stuttering” were relatively robust to two-fold variations in strength for our single somatic cell. The uniqueness of STUT behavior may be due to the anatomical properties and/or just the right combination of channels present in the cell. In addition, the use of an integrate-and-fire model with a prespecified threshold may detract from achieving stuttering-type behavior. For instance, close observation of the electrophysiologic traces for STUT-type cells reveals small bumps during the large gaps where spikes would normally occur. These bumps actually achieve potentials higher than threshold for previous and subsequent AP. A Hudgkin & Hukley like conductance-based model may be needed to capture the subtleties of STUT behavior. A conductance-based model allows for a floating threshold dependent on the state of all the channels included within the model.

In summary, we were able to replicate *in vitro* responses of the GABAergic system by varying combinations of A-type, M-type, and SK-type and proposed SIC channels to a wide range of step currents. Presently underway is a collaboration among the authors to corroborate the proposed channel models using genetic profiles obtained from physiologically characterized interneurons (Fig 3).

### References


1. Gupta, A., Y. Wang, and H. Markram, *Organizing principles for a diversity of GABAergic interneurons and synapses in the neocortex*. Science, 2000. **287**(5451): p. 273-8.

2. Connors, B.W. and M.J. Gutnick, *Intrinsic firing patterns of diverse neocortical neurons*. Trends Neurosci, 1990. **13**(3): p. 99-104.

3. Cajal, R.S., *Histology Due Systeme Nerveux de l'Homme et des Vertebres*. Vol. 2. 1911, Paris.

4. Somogyi, P., et al., *Synaptic connections of morphologically identified and physiologically characterized large basket cells in the striate cortex of cat.* Neuroscience, 1983. **10**(2): p. 261-94.

5. Kisvarday, Z.F., et al., *Synaptic connections of intracellularly filled clutch cells: a type of small basket cell in the visual cortex of the cat.* J Comp Neurol, 1985. **241**(2): p. 111-37.

6. Feldman, M.L. and A. Peters, *The forms of non-pyramidal neurons in the visual cortex of the rat.* J Comp Neurol, 1978. **179**(4): p. 761-93.

7. Martinotti, C., 1889.

8. Markram, H., et al., *Potential for multiple mechanisms, phenomena and algorithms for synaptic plasticity at single synapses.* Neuropharmacology, 1998. **37**(4-5): p. 489-500.

9. Tsodyks, M.V. and H. Markram, *The neural code between neocortical pyramidal neurons depends on neurotransmitter release probability*. Proc Natl Acad Sci U S A, 1997. **94**(2): p. 719-23.

10. Helmchen, F., K. Imoto, and B. Sakmann, *Ca2+ buffering and action potential-evoked Ca2+ signaling in dendrites of pyramidal neurons.* Biophys J, 1996. **70**(2): p. 1069-81.

11. Engel, J., H.A. Schultens, and D. Schild, *Small conductance potassium channels cause an activity- dependent spike frequency adaptation and make the transfer function of neurons logarithmic.* Biophysical Journal, 1999. **76**(3): p. 1310-1319.

12. Kang, J., J.R. Huguenard, and D.A. Prince, *Voltage-gated potassium channels activated during action potentials in layer V neocortical pyramidal neurons.* J Neurophysiol, 2000. **83**(1): p. 70-80.

13. Yamada, W.M., C. Koch, and P.R. Adams, *Multiple channels and calcium dynamics*, in *Methods of Neuronal Modeling: From Ions to Networkds*, C. Koch and I. Segev, Editors. 1998, The MIT Press: Cambridge London. p. 137-170.

14. Hodgkin, A.L. and A.F. Huxley, *A quantitative description of membrane current and its application to conduction and excitation in nerve.* Journal of Physiology-London, 1952. **117**: p. 500-544.

15. Albert, J.L. and J.M. Nerbonne, *Calcium-independent depolarization-activated potassium currents in superior colliculus-projecting rat visual cortical neurons.* J Neurophysiol, 1995. **73**(6): p. 2163-78.

16. Connor, J.A. and C.F. Stevens, *Prediction of repetitive firing behaviour from voltage clamp data on an isolated neurone soma.* J Physiol, 1971. **213**(1): p. 31-53.

17. Neher, E., *Two fast transient current components during voltage clamp on snail neurons.* J Gen Physiol, 1971. **58**(1): p. 36-53.

18. Rudy, B., *Diversity and ubiquity of K channels.* Neuroscience, 1988. **25**(3): p. 729-49.

19. Schwindt, P.C., et al., *Multiple potassium conductances and their functions in neurons from cat sensorimotor cortex in vitro.* J Neurophysiol, 1988. **59**(2): p. 424-49.

20. Spain, W.J., P.C. Schwindt, and W.E. Crill, *Two transient potassium currents in layer V pyramidal neurones from cat sensorimotor cortex.* J Physiol, 1991. **434**: p. 591-607.

21. Storm, J.F., *Action potential repolarization and a fast after-hyperpolarization in rat hippocampal pyramidal cells.* J Physiol, 1987. **385**: p. 733-59.

22. Hoffman, D.A., et al., *K+ channel regulation of signal propagation in dendrites of hippocampal pyramidal neurons.* Nature, 1997. **387**(6636): p. 869-75.

23. Soria, B., *The biophysical basis of K+ channel pharmacology*, in *Ion Channel Pharmacology*, B.S.V. Cena, Editor. 1998, Oxford University Press: Oxford, New York, Tokyo. p. 167-185.

24. Brown, D.A. and P.R. Adams, *Muscarinic suppression of a novel voltage-sensitive K+ current in a vertebrate neurone.* Nature, 1980. **283**(5748): p. 673-6.

25. Brown, D.A., *Ion Channels*. 1988, New York: Plenum. 55-94.

26. Storm, J., *An after-hyperpolarization of medium duration in rat hippocampal pyramidal cells.* J Physiol (Lond), 1989. **409**(1): p. 171-190.

27. Womble, M.D. and H.C. Moises, *Muscarinic inhibition of M-current and a potassium leak conductance in neurones of the rat basolateral amygdala.* J Physiol, 1992. **457**: p. 93-114.

28. Wang, H.S. and D. McKinnon, *Potassium currents in rat prevertebral and paravertebral sympathetic neurones: control of firing properties.* J Physiol, 1995. **485**(Pt 2): p. 319-35.

29. Wang, H.S., et al., *KCNQ2 and KCNQ3 potassium channel subunits: molecular correlates of the M-channel.* Science, 1998. **282**(5395): p. 1890-3.

30. Pineda, J.C., R.S. Waters, and R.C. Foehring, *Specificity in the interaction of HVA Ca2+ channel types with Ca2+-dependent AHPs and firing behavior in neocortical pyramidal neurons.* J Neurophysiol, 1998. **79**(5): p. 2522-34.

31. Foehring, R.C. and D.J. Surmeier, *Voltage-gated potassium currents in acutely dissociated rat cortical neurons.* J Neurophysiol, 1993. **70**(1): p. 51-63.

32. Locke, R.E. and J.M. Nerbonne, *Role of voltage-gated K+ currents in mediating the regular-spiking phenotype of callosal-projecting rat visual cortical neurons.* J Neurophysiol, 1997. **78**(5): p. 2321-35.

33. Lancaster, B. and R.A. Nicoll, *Properties of two calcium-activated hyperpolarizations in rat hippocampal neurones.* J Physiol, 1987. **389**: p. 187-203.

**James B. Maciokas** received his Ph.D. for his work on "Towards an Understanding of the Synergistic properties of Cortical Processing: A Neuronal Computational Modeling Approach" in Phil Goodman's lab at the University of Nevada. He is currently a NEI funded postdoc in Ken Britten's lab at the University of California, Davis using electrophysiological methods to investigate motion processing in awake behaving monkey.